Advances in Remote Sensing, 2016, 5, 103-117
Published Online June 2016 in SciRes. http://www.scirp.org/journal/ars
http://dx.doi.org/10.4236/ars.2016.52009

Scientific Research Publishing

Sensitivity of X-Band (σ^0, γ) and Optical (NDVI) Satellite Data to Corn Biophysical Parameters

Frédéric Baup[1], Lucio Villa[2], Rémy Fieuzal[1], Maël Ameline[1]

[1]Centre d'Etudes de la BIOsphère (CESBIO), Université de Toulouse, CNES/CNRS/IRD/UPS, Toulouse, France
[2]Asociación para la Investigación y el Desarrollo Integral (AIDER), Lima, Perú
Email: frederic.baup@cesbio.cnes.fr

Received 2 March 2016; accepted 12 June 2016; published 15 June 2016

Abstract

The objective of this work was to evaluate the sensitivity of three different satellite signals (interferometric coherence (γ), backscattering coefficient (σ^0) and NDVI) to corn biophysical parameters (leaf area index, height, biomass and water content) throughout its entire vegetation cycle. All of the satellite and *in situ* data were collected during the Multi-spectral Crop Monitoring (MCM'10) experiment conducted in 2010 by the CESBIO Laboratory over eight different agricultural sites located in southwestern France. The results demonstrated that the NDVI is well adapted for leaf area index monitoring, whereas $\gamma_{27.3°}$ is much more suited to the estimation of the three other Biophysical Parameters throughout the entire crop cycle, with a coefficient of determination ranging from 0.83 to 0.99, using non-linear relationships. Moreover, contrary to the use of the NDVI or backscattering coefficients, the use of coherence exhibited a low sensitivity to the changes in vegetation and soil moisture occurring during senescence, offering interesting perspectives in the domain of applied remote sensing.

Keywords

Corn, Biophysical Parameters, Interferometric Coherence, Backscattering Coefficients, NDVI, Terrasar-X, Formosat-2, Spot-4/5

1. Introduction

Corn, which is primarily used for human and animal consumption, is the second-most-produced crop in the world (FAO, http://faostat.fao.org/). As food requirements increase in the future, the monitoring and manage-

How to cite this paper: Baup, F., Villa, L., Fieuzal, R. and Ameline, M. (2016) Sensitivity of X-Band (σ^0, γ) and Optical (NDVI) Satellite Data to Corn Biophysical Parameters. *Advances in Remote Sensing*, **5**, 103-117.
http://dx.doi.org/10.4236/ars.2016.52009

ment of corn crops to meet demand of resources will become a social issue. Satellites offer the possibility to monitor corn worldwide due to their high coverage and high temporal sampling. Among the many choices of operational satellite sensors, this work focuses on three high-resolution optical and radar imagers (pixel size < 20 m) that are able to monitor plots of corn ranging in size from a few to several hundred hectares.

In the optical domain, many studies have highlighted the interest in using satellite data for crop monitoring. These studies have primarily used the Normalized Difference Vegetation Index (NDVI) to estimate crop functioning parameters such as the Leaf Area Index (LAI), yield, soil water demand, fraction of cover, and fraction of active photosynthetic radiation [1]-[4]. The primary drawbacks of these optical approaches are the limited periods of clear skies and the lack of sensitivity to crop geometry/architecture. Fewer studies have addressed crop monitoring in the microwave domain than in the optical domain, and majority of them used C-band data. These studies have explored a wide range of radar signal processing features, such as the backscattering coefficient (σ^0), polarimetric indexes (α angle, entropy, anisotropy) and/or interferometric coherence (γ), for crop classification and crop parameter estimation [5]-[12]. In our knowledge, no studies focused on estimating corn biophysical parameters using SAR images acquired by satellite, particularly at X-band wavelengths.

The combined use of the optical and microwave domains within the electromagnetic spectrum began to increase at the beginning of the 21th century with the launch of synthetic aperture radar (SAR) sensors (such as Envisat, Terrasar-X, Radarsat-2, and Alos), which were in limited use before 2003. Recent studies have demonstrated an interest in combining different sources of satellite data for crop management or monitoring, although there have only been a few studies on this topic [13]-[18]. The primary limitation of such an approach is the lack of a well-adapted dataset that contains both *in situ* and satellite data to better explore the synergistic use of optical and radar remote sensing satellite data, particularly for corn [19] [20].

In this context, the objective of this work is to assess and compare the sensitivity of optical (NDVI) and X-band SAR (backscattering coefficients and interferometric coherence) satellite data to changes in corn biophysical parameters. Four parameters have been defined as target parameters—LAI, height, biomass and water content—which are all considered to be key parameters for food production and water resource management. Whereas the three first parameters can be used to derive the grain yield or leaf nitrogen concentration of the crop (based on empirical or semi-empirical approaches; [2] [21]-[23], the fourth generally serves to quantify the water stress of the plant [24].

This study is based on ground and satellite data acquired during the Multi-spectral Crop Monitoring experiment conducted by the CESBIO Laboratory in 2010 (Section 2) [20]. The methodology is presented in Section 3. The results and discussion are provided in Sections 4 and 5. The conclusion and perspectives are presented in Section 6.

2. Study Site and Data Collection

2.1. Study Site

The study site is located in southwestern France in the Midi-Pyrénées region (coordinates for the center of the area are 43˚29'36"N, 01˚14'14"E) (**Figure 1**). It is strongly anthropized, governed by a temperate climate and primarily conditioned by agricultural activities [20]. During 2010, the annual rainfall reached 600 mm, and the mean daily air temperature ranged from 3.5 to 22˚C. Approximately 10% of the surface is attributed to urban, free water and forest areas. The remaining landscape is composed of grasslands and annual crops (e.g., corn, sunflower, wheat). The eight contrasted studied plots of corn are distributed inside the swath of the satellite images, as illustrated in **Figure 1**. The region of interest is extremely flat, with mean slopes of less than 0.4%, and the soil texture over the 8 studied plots is mainly defined as silty loam (silt = 54.4%, sand = 24.4%, clay = 21.2%), following the USDA classification scheme (**Table 1**). In 2010, corn was sown between April 2nd and May 23rd to be harvested at the beginning of the autumn (from September 7th to October 27th). Plot boundaries were decreased by 10 m to reduce mixel effects.

2.2. Data Collection

Ground and satellite data were obtained from the Multi-spectral Crop Monitoring experiment (MCM'10) conducted in 2010 by the CESBIO Laboratory.

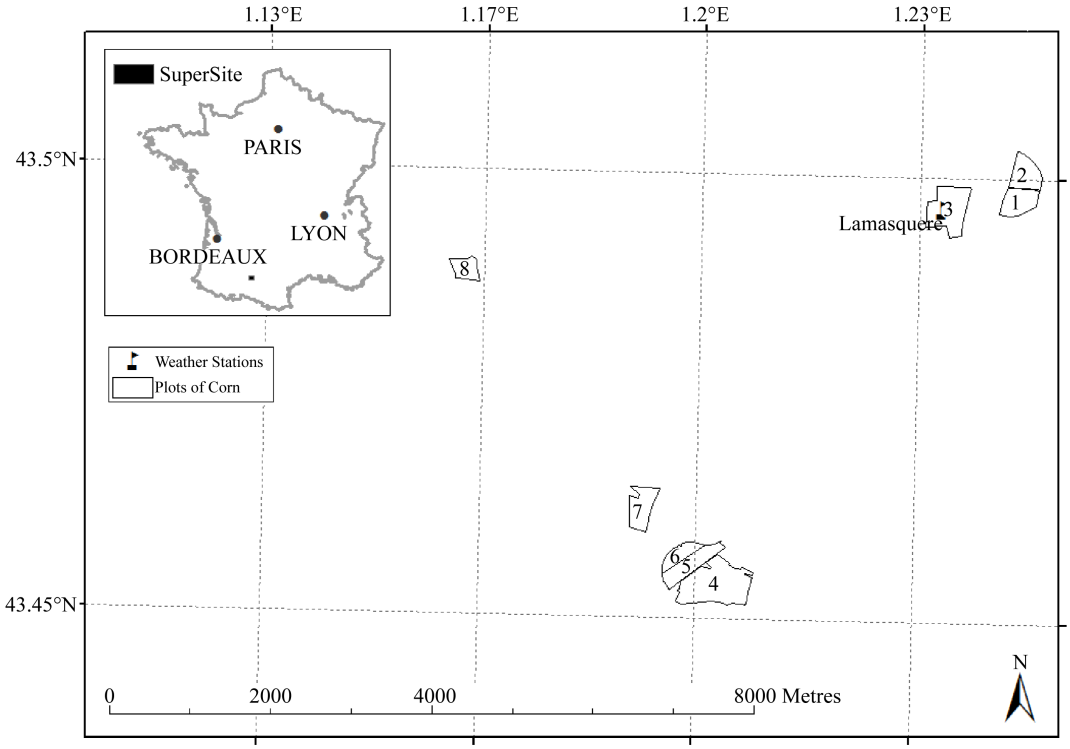

Figure 1. Locations of the eight monitored plots of corn and the climatic station of Lamasquère.

Table 1. Textural and topographic characteristics of the studied plots of corn.

Plot ID	Sand [%]	Silt [%]	Clay [%]	Slope [˚]	Surface [ha]
1	33	51	16	0.07	12.51
2	27	49	24	0.18	13.25
3	13	37	50	0.23	24.02
4	25	58	17	0.78	38.44
5	25	60	15	0.55	14.00
6	22	62	16	0.70	8.34
7	27	56	17	0.28	13.84
8	23	62	15	0.33	7.85

2.2.1. Satellite Data

Twenty Terrasar-X images (X-band, ~9.65 GHz) were acquired from emergence to harvest of the crop (between February 21st and November 24th). The images were delivered at high resolution (pixel spacing ranging from 1 to 3 m) in a Single-look Slant-range Complex (SSC) format from StripMap (SM) and SpotLight (SL) modes and were provided for two contrasting incidence angles (27.3˚ and 53.3˚) (**Table 2**).

Optical images were provided by high-resolution sensors onboard Formosat-2 and Spot-4/5 satellites in the visible to short-wave infrared domains (**Table 2**). The ground spatial resolutions were equal to 8, 20 and 10 m. All of the images were ortho-rectified using CNES ortho-rectification tools. Cloud detection and atmospheric corrections of the Formosat-2 images were applied, and the Spot images were atmospherically corrected using the CNES Kalideos processing chain.

Pre-processing of SAR and optical satellite data are described in **Figure 2**.

Table 2. Primary characteristics of Terrasar-X (TSX), Formosat-2 (F2) and Spot-4/5 images.

Sat	θ (˚)	Pol	Date in 2010 (Month/Day)	Ground range (m)	Azimuth res. (m)
TSX-SM	27.3	HH	0326; 0509; 0520; 0611; 0622; 0703; 0714; 0816; 0929; 1010; 1021	2.44	3.30
TSX-SL	53.3	HH	0305; 0521; 0601; 0612; 0623; 0704; 0715; 0817; 0930	1.47	1.60
F2	±45	-	0410; 0418; 0427; 0521; 0707; 0719; 0731; 0808; 0820; 0827; 0915; 1007	8	8
Spot 4	75; 102	-	0409; 0510; 0605; 0626; 0701; 0711; 0901	20	20
Spot 5	75; 102	-	0410; 0523; 0627; 0920; 0929	10	10

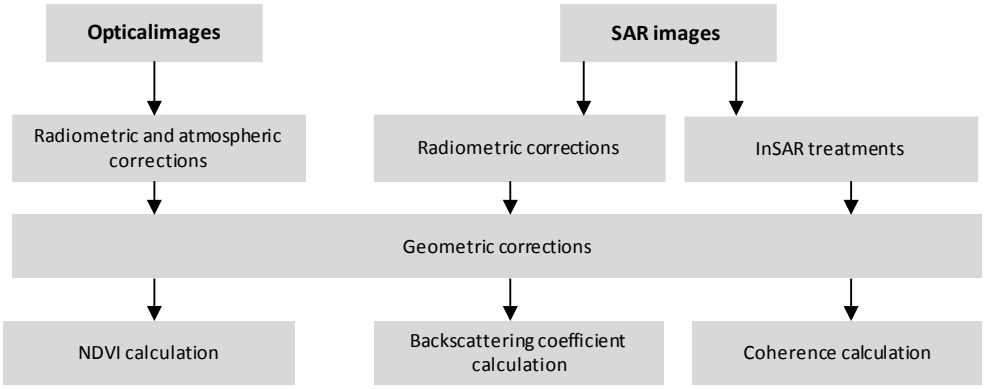

Figure 2. Flow chart of the satellite data pre-processing.

2.2.2. *In Situ* Data

In situ data included measurements of surface soil roughness, inter-row distance, Crop Height (CH), above-ground Crop Dry and Fresh Biomass (CDB and CFB, respectively), Crop Water Content (CWC) and Surface Soil Moisture (SSM).

The two first parameters were considered stable over time (*i.e.*, during the crop growth cycle). Soil roughness was measured using a 2-m pin profilometer, and the mean statistical parameters were calculated immediately after sowing, when the soil was smooth (h_{rms} = 1.2 cm, l_c = 4.5 cm). The inter-row distance was constant between the plots and was equal to 80 cm.

The four remaining parameters, which vary substantially over space and time, were collected throughout the vegetation cycle, from emergence to harvest. The dielectric constant of the soil was measured using mobile theta probe sensors, and the volumetric soil moisture of the first five centimeters was estimated using an *in situ* calibration function (R^2 = 0.75, RMSE = 4.1%, n = 403, [20]). For the 8 plots, the mean SSM value ranged between 9 and 29% $m^3 \cdot m^{-3}$ throughout the crop cycle.

The mean vegetation height was derived from measurements performed over more than ten samples for each plot. Plant height reached its maximum value (approximately 3.5 m) 100 days (on average) after sowing (**Figure 3**).

Regular biomass measurements were performed during the corn agricultural season over two plots (plot ID #7 and #8). For each date, five samples were weighed to obtain the fresh biomass, dried in an oven, and reweighed to determine the dry biomass. The total crop water content (including leaves, stems, and fruit) was derived from the difference between the CFB and the CDB, and the values were related to the phenological cycle of the crop. From emergence to flowering (approximately on DOY #220), the water content reached a maximum of 80% and decreased during senescence, reaching 50% only a few days before being harvested (the WC of the fruit was less than 30%).

All of the *in situ* variables were collected quasi-synchronously with satellite acquisitions (a mean time lag of less than 1 day was observed).

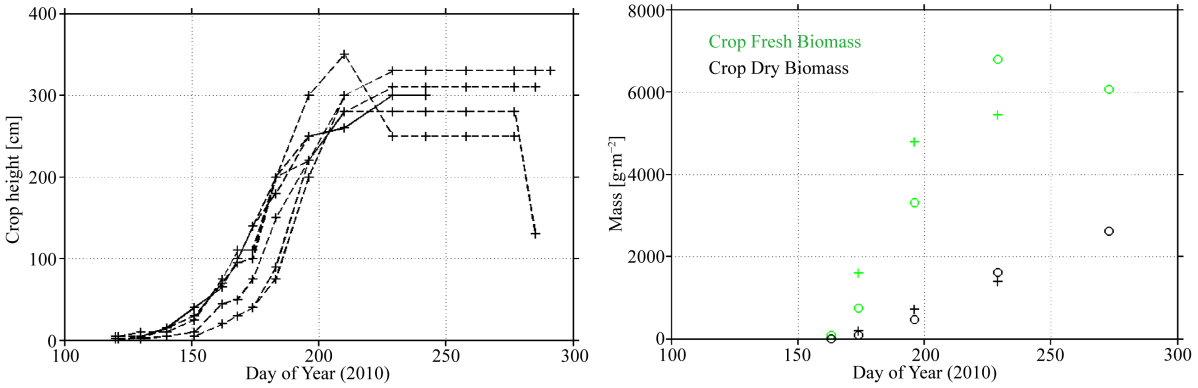

Figure 3. Temporal change in crop height over the 8 plots of corn (a) and in the fresh and dry biomass (b) measured over plot ID #7 (cross marker) and #8 (circle marker).

3. Methodology

Among the wide choice of Biophysical Parameters (BP), the proposed methodology focuses on the relationships estimated between crop and soil parameters (LAI, CH, CFB, CDB, CWC, and SSM), and three satellite indicators for the entire crop cycle: NDVI, $\gamma_{27.3^\circ}$, $\gamma_{53.3^\circ}$, $\sigma^0_{\mathrm{HH}-27.3^\circ}$ and $\sigma^0_{\mathrm{HH}-53.3^\circ}$ (Equation (1)).

$$BP = a_{BP} \cdot \mathrm{e}^{-b_{BP} \cdot \text{satellite indicators}} + c_{BP} \tag{1}$$

where *BP* represents the biophysical parameter under consideration (LAI, CH, CFB, CDB, CWC and SSM), and a_{BP}, b_{BP} and c_{BP} are the associated empirical parameters.

The relationships between biomass (wet and dry), crop water content, crop height, LAI surface soil moisture content and satellite signals were evaluated. The NDVI was estimated from three optical satellites (Formosat-2, Spot-4/5). The similarity of the NDVI values was determined by comparing the values estimated by each satellite from images acquired at the same time ($\mathrm{R}^2_{\mathrm{NDVI(Spot4/F2)}} = 0.99$, $\mathrm{R}^2_{\mathrm{NDVI(Spot5/F2)}} = 0.99$, $\mathrm{R}^2_{\mathrm{NDVI(Spot4/Spot5)}} = 0.99$).

The backscattering coefficients of the Terrasar-X images (SL and SM modes) were estimated using the radiometric calibration procedure given in [16] and performed using NEST (Next ESA SAR Toolbox) software. Backscattering coefficients acquired at HH polarization (σ^0_{HH}) were derived from the digital number (DN) of the pixel (*i*), the calibration factor (*K*) and the incidence angle (θ) (Equation (2)).

$$\sigma_i^0(\mathrm{dB}) = 20 \cdot \log(DN_i) + 10 \cdot \log(K) + 10 \cdot \log(\sin(\theta_i)) \tag{2}$$

Geocoded interferometric coherence images were calculated from InSAR treatment processing based on the approach described in [25] and using open-source software, namely, DORIS (Delft Object-oriented Radar Interferometric) and ADORE (Automated DORIS Environment). Master and slave images were defined for each SAR mode (SM and SL) to calculate the coherence coefficients (γ) over the slave images, following Equation (3):

$$\gamma = \left| \frac{\frac{1}{N}\sum_{i=0}^{N} M_i \cdot S_i^*}{\frac{1}{N}\sum_{i=0}^{N} M_i \cdot M_i^* \cdot \frac{1}{N}\sum_{i=0}^{N} S_i \cdot S_i^*} \right| \tag{3}$$

where M_i and S_i represent the value of the pixel *i* of the master and slave images, respectively, M_i^* and S_i^* denote the complex conjugate matrix, and N denotes the total number of analysed pixels.

As described in [26], decorrelation sources can be separated in four factors: $\gamma = \gamma_{\mathrm{thermal}} \cdot \gamma_{\mathrm{geometrical}} \cdot \gamma_{\mathrm{volume}} \cdot \gamma_{\mathrm{temporal}}$. Thermal decorrelation can be neglected for high signal-to-noise ratio [27] [28]. Geometric decorrelation was reduced by applying a spectral filter, and the spatial baselines of all of the Insar pairs were verified as being lower than their critical baselines (**Table 3**). Volumetric and temporal coherences cannot be separated as a simple sum of independent coefficients. As demonstrated and modelled by [29], the second component is more affected by the vertical change in vegetation. Therefore, we used the coherence coefficient to estimate the crop

Table 3. Summary of interferometric parameters for the two considered modes (SM and SL) for each pair of master and slave images: critical baseline ($B_{critical}$), perpendicular (B_{perp}), parallel baseline (B_{par}) and temporal baseline (B_{temp}).

Interferometric pair (master-slave)	$B_{critical}$ (m)	B_{perp} (m)	B_{par} (m)	B_{temp} (days)
		Stripmap Mode		
03/26-05/09	4477	121.4	103.7	44
05/09-05/20	4479	−49.4	−18.6	11
05/20-06/11	4479	98.7	47.8	22
06/11-06/22	4479	−155.1	−59.8	11
06/22-07/03	4479	−124.9	−56.1	11
07/03-07/14	4480	87.7	47.3	11
07/14-06/16	4480	−16.9	−33.6	33
08/16-09/29	4479	−259.9	−88.7	44
09/29-10/10	4480	274.1	106.5	11
10/10-10/21	4479	−121.8	−94.2	11
		Spotlight Mode		
03/05-05/21	13939	239.9	337.5	77
05/21-06/01	13941	−33.7	−32.6	11
06/01-06/12	13941	84.4	94.1	11
06/12-06/23	13941	−112.2	−102.2	11
07/04-07/15	13942	61.7	74.2	11
07/15-08/17	13942	40.3	4.9	33
08/17-09/30	13941	−155.2	−223.5	44

biophysical parameters over time.

Ten and seven coherence images were generated in the StripMap and SpotLight modes, respectively. All of the images were geo-referenced using ortho-photos (spatial resolution of 50 cm) provided by the French National Geographic Institute, and the final location accuracy was less than 2 pixels, on average, considering the different products. Examples of NDVI, γ and σ^0_{HH} images are provided in **Figure 4** for a sub-area of the study site from May 2010.

4. Results

4.1. Influence of Surface Soil Moisture

The first results confirmed that no accurate empirical relationships could be estimated between the surface soil moisture changes and the satellite signals over the entire vegetation phenological cycle ($0 < R^2 < 0.13$) (**Table 4**). These weak correlations are attributed to the fact that the satellite signals were mainly acquired in the presence of vegetation. In these conditions, the X-band and optical electromagnetic waves did not penetrate through the vegetation layer but mainly interacted with the upper layer of the crop (*i.e.*, leaves, stems, flowers) and not with the SSM. Nevertheless, according to [30] [31], stronger correlations can be observed when the soil is bare, from sowing to the first phenological stages of corn.

4.2. Sensitivity of Satellite Signal to LAI

The values of the statistical parameters associated with the relationships estimated between the LAI and satellite signals were disparate. The results associated with the optical signal confirmed that NDVI is well suited for LAI

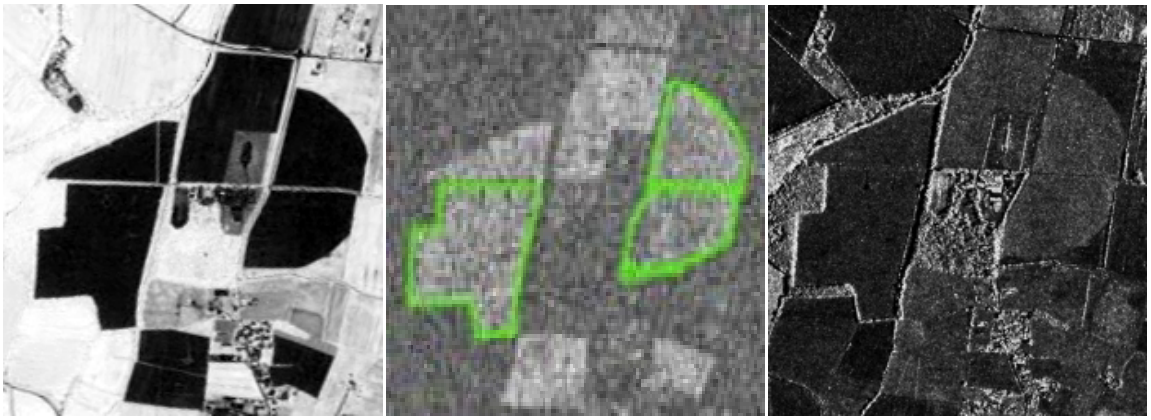

(a) (b) (c)

Figure 4. Examples of NDVI (a), γ (SM mode, (b) and σ^0_{HH} (c) images extracted from the study site acquired on May 21st and 20th, 2010. Plots of corns (IDs #1, 2 and 3) are outlined in green.

Table 4. Values of the empirical parameters (a_{SSM}, b_{SSM} and c_{SMM}) used to determine the SSM, number of data points used (n), coefficients of determination (R^2_{SSM}), and absolute and relative root mean square errors ($RMSE_{SSM}$ and $rRMSE_{SSM}$, respectively).

	a_{SSM}	b_{SSM}	c_{SSM}	n	R^2_{SSM}	$RMSE_{SSM}$	$rRMSE_{SSM}$
	-	-	-	-	-	[%Vol.]	[%]
NDVI	−0.9659	0.0597	0.9481	132	0.13	6.9	36
$\sigma^0_{27.3^\circ}$	−1.8164	0.0814	−7.3822	61	0.04	7.4	36
$\sigma^0_{53.3^\circ}$	−48.1308	0.0032	35.1473	64	0.13	7.0	38
$\gamma_{27.3^\circ}$	1.6134	0.002	−0.9049	53	0.07	17.2	90
$\gamma_{53.3^\circ}$	−655.3122	0.8207	0.5918	43	0.08	6.7	36

retrieval, as previously noted in several studies [2]. The radar signals (either backscattering coefficients or interferometric coherence) exhibited contrasting performances, with R^2 values ranging from 0.03 to 0.51 (**Table 5**). According to the relationships based on the backscattering coefficients, the performances depended on the considered sensor configuration, with higher R^2 values associated with a high incidence angle (53.3˚ in this case). This result appears consistent with previous studies [32], showing that the sensitivity of the backscattering coefficients to soil and vegetation parameters depend on the considered incidence angle.

4.3. Sensitivity of Satellite Signal to Biomass and Crop Water Content

The performances associated with the relationships between corn biomass and satellite signals showed similar trends regardless of the considered fraction of the crop (CFB, CDB and CWC) (**Table 6**). The poorest values of R^2 were obtained for the optical index (NDVI) or backscattering coefficients (regardless of the incidence angle), with values never exceeding 0.37, whereas the highest R^2 values were obtained using interferometric coherences (regardless of the incidence angle), with values of R^2 close to 0.99. Despite these strong correlations, the application of these relationships is limited to the first phenological stages of corn due to the early saturation of the interferometric coherence (**Figure 5**). The results demonstrated that the saturation of the coherence occurred at a later phenological stage with the decrease in incidence angle, regardless of the considered crop parameter (CFB, CDB and CWC). For example, the saturation level was close to 1080 g·m^{-2} using $\gamma_{53.3^\circ}$ (beginning of stage 1: leaf development, BBCH), whereas this level reached 1738 g·m^{-2} using $\gamma_{27.3^\circ}$ (end of stage 3: stem elongation, BBCH) for the CFB.

Table 5. Values of the empirical parameters (aLAI, bLAI and cLAI) used to determine the LAI, number of data points used (n), coefficients of determination (R^2_{LAI}), and absolute and relative root mean square errors (RMSELAI and rRMSELAI, respectively).

	a_{LAI}	b_{LAI}	c_{LAI}	n_{LAI}	R^2_{LAI}	$RMSE_{LAI}$	$rRMSE_{LAI}$
	-	-	-	-	-	$[m^2 \cdot m^{-2}]$	[%]
NDVI	−1.1022	0.6154	0.9621	132	0.98	0.12	5
$\sigma^0_{27.3^\circ}$	−9.8493	5.5725	−7.6989	61	0.03	1.61	80
$\sigma^0_{53.3^\circ}$	−15.2904	2.5499	−9.1145	64	0.51	1.12	66
$\gamma_{27.3^\circ}$	0.2426	1.2499	0.6061	53	0.44	1.09	56
$\gamma_{53.3^\circ}$	0.0915	1.0964	0.5678	43	0.18	1.17	57

Table 6. Values of the empirical parameters (a, b and c) used to determine the fresh biomass, dry biomass and biomass water content, number of data used (n), coefficients of determination (R^2), and absolute and relative root mean square errors (RMSE and rRMSE, respectively). Linear relationships were applied when the value of c was not provided.

		a	b	c	n	R^2	RMSE	rRMSE
		-	-	-	-	-	$[g \cdot m^{-2}]$	[%]
Fresh Biomass	NDVI	−0.9573	0.0013	0.752	26	0.27	2878	61
	$\sigma^0_{27.3^\circ}$	−0.0001	−7.3844	-	11	0.07	7828	214
	$\sigma^0_{53.3^\circ}$	0.0002	−10.0205	-	11	0.17	4766	127
	$\gamma_{27.3^\circ}$	0.134	0.0013	0.6105	11	0.99	1469	40
	$\gamma_{53.3^\circ}$	0.0543	0.0021	0.5842	8	0.99	2665	74
Dry Biomass	NDVI	20.7021	0	−19.9434	26	0.04	-	-
	$\sigma^0_{27.3^\circ}$	0.0001	−7.7324	-	11	0.02	7663	807
	$\sigma^0_{53.3^\circ}$	0.0005	−9.8427	-	11	0.26	1609	166
	$\gamma_{27.3^\circ}$	0.1379	0.011	0.6104	11	0.99	1025	108
	$\gamma_{53.3^\circ}$	0.0553	0.0169	0.5842	8	0.99	1064	119
Biomass Water Content	NDVI	−0.4873	0.0003	0.8966	26	0.37	1897	53
	$\sigma^0_{27.3^\circ}$	−0.0002	−7.1376	-	11	0.22	2790	103
	$\sigma^0_{53.3^\circ}$	0.0002	−9.8444	-	11	0.08	5126	185
	$\gamma_{27.3^\circ}$	0.1338	0.0015	0.6102	11	0.99	997	37
	$\gamma_{53.3^\circ}$	0.0541	0.0024	0.5843	8	0.99	1692	62

4.4. Sensitivity of Satellite Signal to Height

Accurate estimates of corn height were obtained from relationships based on the NDVI, interferometric coherence at 27.3˚ and backscattering coefficients at 53.3˚ (**Table 7**). The relationships between CH and $\gamma_{27.3^\circ}$ exhibited the best statistical index value, with R^2 values greater than 0.8 and a maximum rRMSE of the corn height estimates of 32%. The performance of the other indicators decreased gradually for relations based on $\sigma^0_{HH-53.3^\circ}$, NDVI, $\gamma_{53.3^\circ}$, and $\sigma^0_{HH-27.3^\circ}$. The associated R^2 and rRMSE values ranged from 0.71 to 0.04 and from 78 to 102%, respectively.

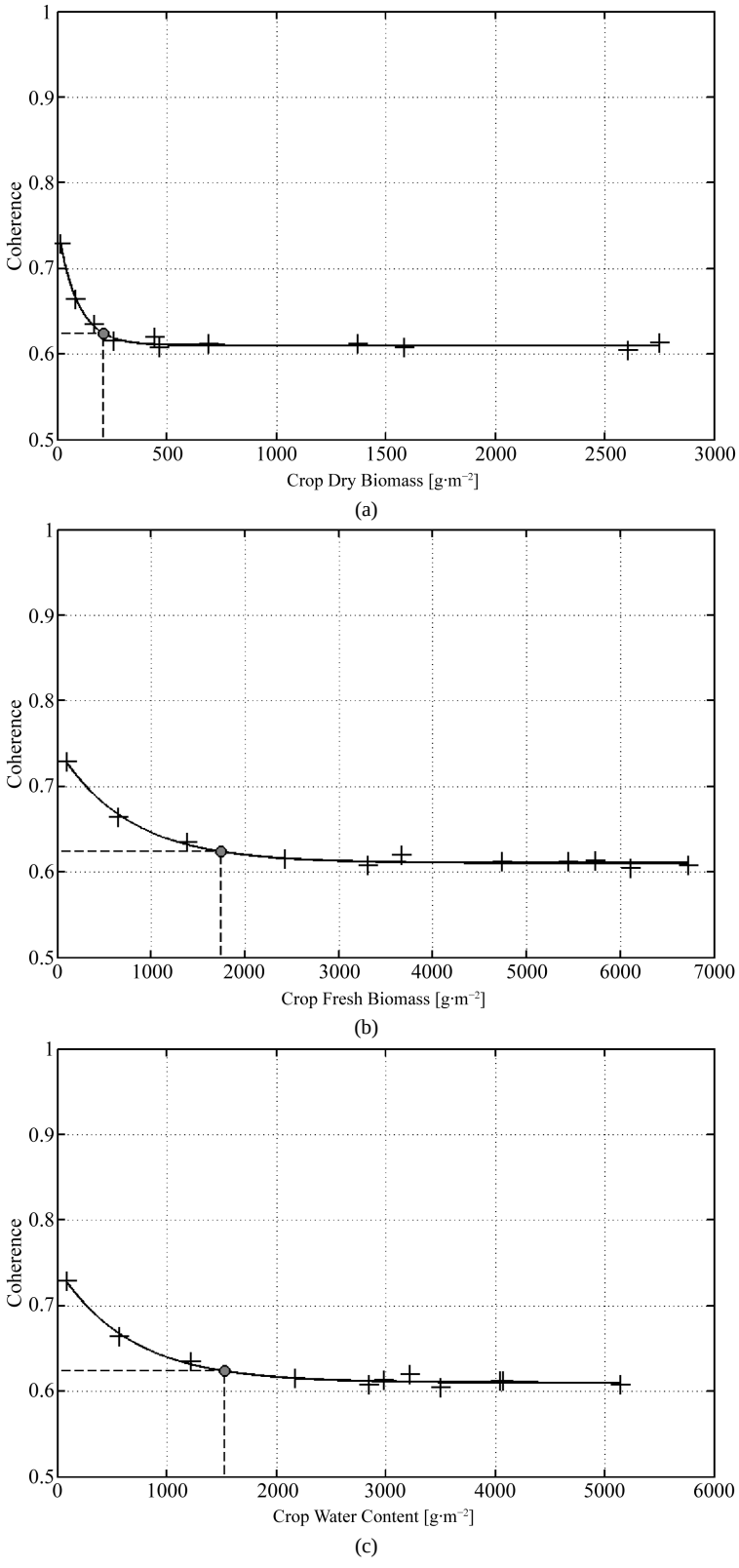

Figure 5. Estimated relationships between the corn dry biomass (a), fresh biomass (b), water content (c) and interferometric coherence acquired at 27.3˚. Ninety percent of signal sensitivity is marked by vertical and horizontal dotted black lines for each sub-plot.

Table 7. Values of the empirical parameters (aCH, bCH and cCH) used to determine the corn height, number of data used (n), coefficients of determination (R^2_{CH}), and absolute and relative root mean square errors (RMSECH and rRMSECH, respectively).

	a_{CH}	b_{CH}	c_{CH}	n	R^2_{CH}	$RMSE_{CH}$	$rRMSE_{CH}$
	-	-	-	-	-	[cm]	[%]
NDVI	−0.6268	0.0137	0.7464	132	0.67	116	78
$\sigma^0_{27.3^\circ}$	−0.5738	0.0524	−7.7085	61	0.04	234	102
$\sigma^0_{53.3^\circ}$	−5.7431	0.0307	−9.1702	64	0.71	110	92
$\gamma_{27.3^\circ}$	0.2024	0.0157	0.6084	53	0.83	56	32
$\gamma_{53.3^\circ}$	0.2071	0.0445	0.5698	43	0.61	166	94

These observations can be interpreted based on the configuration of the X-band data and the associated sensitivity. The sensitivity of backscattering coefficients are influenced more by vegetation in images acquired at high incidence angles (>30˚) than at low incidence angles due to volume and double bounce contributions. At low incidence angles, backscattering coefficients are influenced more by a single scattering mechanism due to the soil contribution (associated with soil moisture and soil roughness changes). Thus, the correlation with crop height is lower at a low incidence angle than at a high incidence angle. According to the coherence, the low-incidence images are more strongly correlated with crop height, which is contrary to the results obtained from the backscattering coefficients (where soil moisture values more strongly affect the signal). An explanation of this phenomenon is that as the crop grows, the soil contribution decreases ($R^2 < 0.13$ between coherence and SSM) with the increase in vegetation contribution, which decorrelates more rapidly than soil, especially close to the nadir (27.3˚), where the vertical dynamic of the vegetation layer strongly affects the coherence. The decrease in the coherence over time can be attributed to the vegetation layer and not to the soil, which is expected to be coherent for an interval of a few days. The overall pattern of coherence decreases with the increase in crop height until saturation, inducing an increase in incoherent scattering mechanisms (**Figure 6**). The non-linear shape of the relationship can be explained by the progressive decrease in the soil contribution (for which the correlation is high), to the benefit of the incoherent vegetation contribution.

Figure 6 presents the best results obtained with optical and X-band satellite data. The relationships indicate comparable behaviors with two different periods: (i) a high sensitivity with an exponential decrease in the case of interferometric coherence and an exponential increase for the NDVI and backscattering coefficients, and (ii) a signal saturation phase for height values depending on the satellite signal under consideration. This level of saturation (highlighted in **Figure 6** by the point located at 90% of the overall relationship saturation) is reached for corn heights near 75, 150 and 160 cm for the relationships based on backscattering coefficients, interferometric coherence and NDVI, respectively. **Figure 6** also illustrates that surface changes (SSM, CWC, phenological stage), which occurred after 90% signal saturation, have a smaller effect on the coherence relationship than on the relationships based on the backscattering coefficients and/or NDVI. In addition, the results (figure not shown here) confirmed that parallel and/or perpendicular baselines values do not affect the values of coherence because they are inferior to the critical baseline.

5. Discussion

As expected, none of the tested satellite signals can be used to estimate the surface soil moisture changes throughout the vegetation cycle, especially when the presence of the vegetation layer masks the soil layer. This well-known phenomenon can be explained by the low penetration depth of the wavelength (both in optical and X-band frequencies) into the crop layer. The estimation of SSM under the crop layer remains challenging and is presently investigated using the POLSAR technique (giving access to the double bounce mechanism, partially associated with the SSM) or L-band signals (offering higher penetration depth and thus a stronger correlation with SSM) [33] [34]. The results obtained in this paper confirm that techniques based only on backscattering coefficients, coherence or optical signals are not well adapted for monitoring SSM under the crop layer, and they reinforce the interest in developing new approaches such as those proposed by [34]. However, the weak correla-

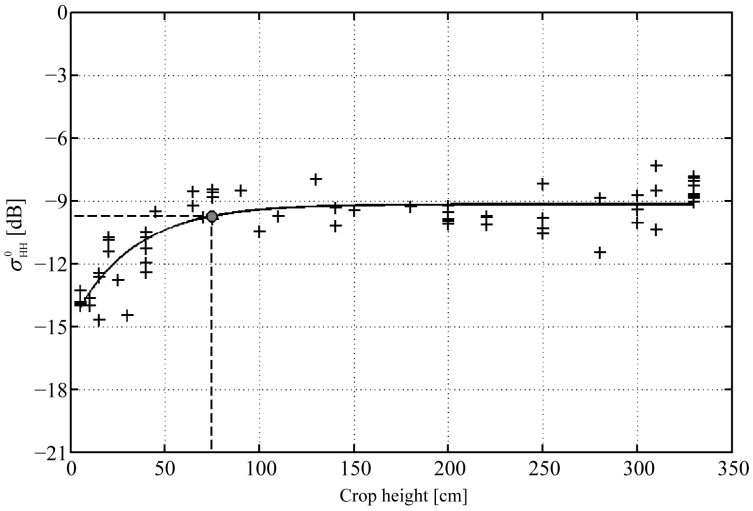

(a)

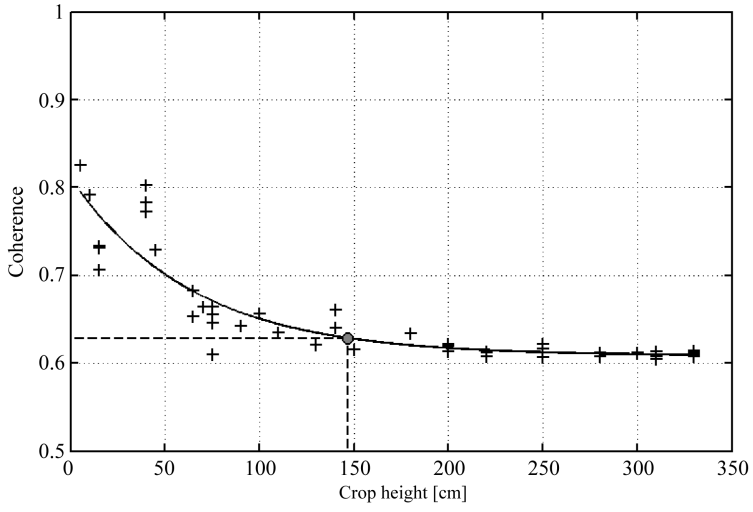

(b)

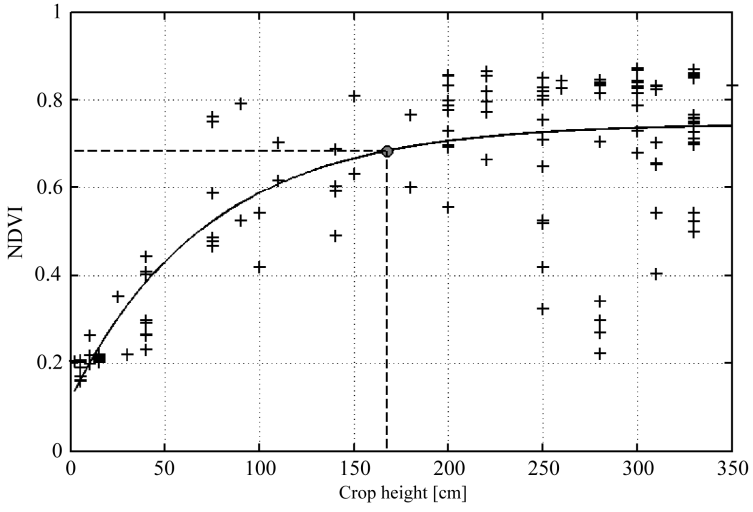

(c)

Figure 6. Estimated relationships between corn height and backscattering coefficients (a), interferometric coherence (b) and NDVI (c); 90% sensitivity is marked by vertical and horizontal dotted black lines for each sub-plot.

tions obtained between the satellite signals and SSM values indicate that the empirical relationships estimated between the biophysical parameters of the vegetation (CDB, CFB, LAI and height) and the satellite signals are slightly influenced by variation in SSM.

The analyses of the relationships estimated between the satellite signals and the vegetation parameters revealed several important points. First, the results showed that among all of the tested satellite signals, optical data appear more suited to monitor the LAI of corn with sufficient confidence. Considering X-band signals, only the backscattering coefficient acquired at high incidence angle (53.3˚) could justifiably be used to estimate the LAI (with lower confidence than with optical data). Therefore, the monitoring of corn should be performed using a multi-temporal approach mainly based on optical data and partially composed of radar data, the latter being used only to replace optical data in case of cloud cover. Under these conditions, the combine use of optical and radar data could be used to accurately estimate some variables strongly correlated with the LAI, such as leaf transpiration, the interaction with the radiation by the leaf, and latent and sensible heat fluxes [35] [36].

The second part of the results demonstrated that the dry or fresh biomass and crop water content are strongly correlated over time. Consequently, considering that crop water content is a key parameter in the management of agricultural crops, the monitoring of dry or fresh biomass could be investigated to further estimate the water content of the crop, particularly to determine the maturity of the crop before harvest [37]. Concerning the estimates of CDB, CFB and CWC, the best correlations were achieved using the coherence estimated from images acquired at 27.3˚ (R^2 = 0.99). Although these relationships quickly saturated (for values of fresh biomass close to 1738 $g \cdot m^{-2}$), the results (**Figure 5**) demonstrated that coherence is strongly sensitive to the first phenological stages of the crop (from emergence to the end of the stem elongation, as defined in the BBCH classification), contrary to other satellite signals, which were too strongly affected by SSM changes during the bare soil period or by the color changes and decrease in CWC during senescence. This accurate and early detection of the first phenological stages could be then implemented to estimate crop yields by using an agro-meteorological model, as demonstrated by [2] [38]-[42].

The estimate of CH demonstrated the potential of using the coherence instead of the other satellite signals, especially from images acquired at low incidence angle (27.3˚). Consequently, the coherence values could be implemented in empirical and/or semi-empirical methods for predicting yields as demonstrated by [21] [22]. Moreover, the estimate of CH could be used as a key parameter in land-use mapping to more precisely differentiate similar crops where architectural differences mainly accrue from height differences [43]. For example, the method could be investigated to improve corn and sorghum classification given their heights of approximately 1 and 3 m, respectively, over the study region.

6. Conclusions

This study evaluated the sensitivity of three sources of satellite data (X-band backscattering coefficients, interferometric coherence, and NDVI) to crop parameters over an entire vegetation cycle. The first part of the results demonstrated that the SSM changes were not correlated with satellite signals due to the presence of vegetation and the low penetration depth of the electromagnetic wave into the crop layer (regardless of the spectral domain). Consequently, we demonstrated that SSM did not significantly affect the relationships estimated between the satellite signals and the vegetation components (CDB, CFB, LAI and height). The second part of the results demonstrated that the LAI of corn can be estimated well using the NDVI (as was known from previous studies) and partially substituted by the use of backscattering coefficients acquired at a high incidence angle (53.3˚). The results also demonstrated the potential of using the coherence acquired at a low incidence angle (despite the early saturation of the coherence) to estimate the dry or fresh biomass and the water content, especially for the first phenological stages of the corn (R^2 = 0.99). The best corn height estimates were obtained by considering the interferometric coherence extracted from the images acquired at a low incidence angle (27.3˚) due to its higher decorrelation effects. In this case, crop height can be accurately estimated before 150 cm (R^2 = 0.83, RMSE = 56 cm, rRMSE = 32%). The use of backscattering coefficients at a high incidence angle and the use of NDVI were less accurate, even though the coefficients of determination were higher than 0.67 (the relative errors, which ranged between 78 and 92%, are still important). Moreover, the use of coherence is of particular interest for monitoring vegetation parameters because it is less sensitive to SSM and CWC than are σ^0 or NDVI during senescence.

In the near future, these relationships could be used in empirical or semi-empirical approaches to estimate

crop yield at the landscape scale as presented in the "Discussion" section. Moreover, these results must be extended to other optical and X-band satellite missions such as Sentinel-2, COSMO-SkyMed, TamDEM-X and PAZ.

Acknowledgements

The authors wish to thank DLR for providing TerraSAR images (DLR-HYD0611), the Delft Institute of Earth Observation and Space Systems for providing access to DORIS and Mr. Batuhan Osmanoglu for his help in signal processing (ADORE software). We also thank the CNES for its funding and the people who helped with the ground measurements and the farmers for their time and availability.

References

[1] Mkhabela, M.S., Bullock, P., Raj, S., Wang, S. and Yang, Y. (2001) Crop Yield Forecasting on the Canadian Prairies Using MODIS NDVI Data. *Agricultural and Forest Meteorology*, **151**, 385-393. http://dx.doi.org/10.1016/j.agrformet.2010.11.012

[2] Claverie, M., Demarez, V., Duchemin, B., Hagolle, O., Ducrot, D., Marais-Sicre, C., Dejoux, J.F., Huc, M., Keravec, P., Béziat, P., Fieuzal, R., Ceschia, E. and Dedieu, G. (2012) Maize and Sunflower Biomass Estimation in Southwest France Using High Spatial and Temporal Resolution Remote Sensing Data. *Remote Sensing of Environment*, **124**, 844-857. http://dx.doi.org/10.1016/j.rse.2012.04.005

[3] Johnson, D.M. (2014) An Assessment of Pre- and Within-Season Remotely Sensed Variables for Forecasting Corn and Soybean Yields in the United States. *Remote Sensing of Environment*, **141**, 116-128. http://dx.doi.org/10.1016/j.rse.2013.10.027

[4] Kross, A., McNairn, H., Lapen, D., Sunohara, M. and Champagne, C. (2015) Assessment of RapidEye Vegetation Indices for Estimation of Leaf Area Index and Biomass in Corn and Soybean Crops. *International Journal of Applied Earth Observation and Geoinformation*, **34**, 235-248. http://dx.doi.org/10.1016/j.jag.2014.08.002

[5] Bouman, B.A.M. and van Kasteren, H.W.J. (1990) Ground-Based X-Band (3-cm Wave) Radar Backscattering of Agricultural Crops. II. Wheat, Barley, and Oats; the Impact of Canopy Structure. *Remote Sensing of Environment*, **34**, 107-119. http://dx.doi.org/10.1016/0034-4257(90)90102-R

[6] Wegmuller, U. and Werner, C. (1997) Retrieval of Vegetation Parameters with SAR Interferometry. *IEEE Transactions on Geoscience and Remote Sensing*, **35**, 18-24. http://dx.doi.org/10.1109/36.551930

[7] Engdahl, M.E., Borgeaud, M. and Rast, M. (2001) The Use of ERS-1/2 Tandem Interferometric Coherence in the Estimation of Agricultural Crop Heights. *IEEE Transactions on Geoscience and Remote Sensing*, **39**, 1799-1806. http://dx.doi.org/10.1109/36.942558

[8] Blaes, X. and Defourny, P. (2003) Retrieving Crop Parameters Based on Tandem ERS 1/2 Interferometric Coherence Images. *Remote Sensing of Environment*, **88**, 374-385. http://dx.doi.org/10.1016/j.rse.2003.08.008

[9] Prasad, R. (2009) Retrieval of Crop Variables with Field-Based X-Band Microwave Remote Sensing of Ladyfinger. *Advances in Space Research*, **43**, 1356-1363. http://dx.doi.org/10.1016/j.asr.2008.12.017

[10] Lopez-Sanchez, J.M. and Ballester-Berman, J.D. (2009) Potentials of Polarimetric SAR Interferometry for Agriculture Monitoring. *Radio science*, **44**, 1-20. http://dx.doi.org/10.1029/2008RS004078

[11] Santoro, M., Wegmuller, U. and Askne, J.I.H. (2010) Signatures of ERS-Envisat Interferometric SAR Coherence and Phase of Short Vegetation: An Analysis in the Case of Maize Fields. *IEEE Transactions on Geoscience and Remote Sensing*, **48**, 1702-1713. http://dx.doi.org/10.1109/TGRS.2009.2034257

[12] Lopez-Sanchez, J.M., Hajnsek, I. and Ballester-Berman, J.D. (2012) First Demonstration of Agriculture Height Retrieval with PolInSAR Airborne Data. *IEEE Geoscience and Remote Sensing Letters*, **9**, 242-246. http://dx.doi.org/10.1109/LGRS.2011.2165272

[13] Dabrowska-Zielinska, K., Inoue, Y., Kowalik, W. and Gruszczynska, M. (2007) Inferring the Effect of Plant and Soil Variables on C- and L-Band SAR Backscatter over Agricultural Fields, Based on Model Analysis. *Advances in Space Research*, **39**, 139-148. http://dx.doi.org/10.1016/j.asr.2006.02.032

[14] Baghdadi, N., Boyer, N., Todoroff, P., El Hajj, M. and Bégué, A. (2009) Potential of SAR Sensors TerraSAR-X, ASAR/ENVISAT and PALSAR/ALOS for Monitoring Sugarcane Crops on Reunion Island. *Remote Sensing of Environment*, **113**, 1724-1738. http://dx.doi.org/10.1016/j.rse.2009.04.005

[15] Hadria, R., Duchemin, B., Baup, F., Le Toan, T., Bouvet, A., Dedieu, G. and Le Page, M. (2009) Combined Use of Optical and Radar Satellite Data for the Detection of Tillage and Irrigation Operations: Case Study in Central Morocco. *Agricultural Water Management*, **96**, 1120-1127. http://dx.doi.org/10.1016/j.agwat.2009.02.010

[16] Fieuzal, R., Baup, F. and Marais-Sicre, C. (2013) Monitoring Wheat and Rapeseed by Using Synchronous Optical and Radar Satellite Data—From Temporal Signatures to Crop Parameters Estimation. *Advanced in Remote Sensing*, **2**, 162-180. http://dx.doi.org/10.4236/ars.2013.22020

[17] McNairn, H., Kross, A., Lapen, D., Caves, R. and Shang, J. (2014) Early Season Monitoring of Corn and Soybeans with TerraSAR-X and RADARSAT-2. *International Journal of Applied Earth Observation and Geoinformation*, **28**, 252-259. http://dx.doi.org/10.1016/j.jag.2013.12.015

[18] Fieuzal, R. and Baup, F. (2016) Monitoring Sunflower by Using Synchronous Optical and Radar Satellite Data: From Temporal Signatures to Crop Parameters Estimation. Accepted for publication by the International Journal of Remote Sensing.

[19] AgriSAR (2008) Final Report of ESA Contract "AGRISAR 2006 Agricultural Bio-/Geophysical Retrievals from Frequent Repeat SAR and Optical Imaging". Report ID #19974/06/I-LG, Version 1. https://earth.esa.int/c/document_library/get_file?folderId=21020&name=DLFE-397.pdf

[20] Baup, F., Fieuzal, R., Marais-Sicre, C., Dejoux, J.F, le Dantec, V., Mordelet, P., Claverie, M., Hagolle, O., Lopes, A., Keravec, P., Ceschia, E., Mialon, A. and Kidd, R. (2012) MCM'10: An Experiment for Satellite Multi-Sensors Crop Monitoring from High to Low Resolution Observations. *IEEE International Geoscience and Remote Sensing Symposium*, Munich, 22-27 July 2012, 4849-4852. http://dx.doi.org/10.1109/igarss.2012.6352527

[21] Yin, X., McClure, M.A. and Hayes, R.M. (2011) Improvement in Regression of Corn Yield with Plant Height Using Relative Data. *Journal of the Science of Food and Agriculture*, **91**, 2606-2612. http://dx.doi.org/10.1002/jsfa.4477

[22] Yin, X., Hayes, R.M., McClure, M.A. and Savoy, H.J. (2012) Assessment of Plant Biomass and Nitrogen Nutrition with Plant Height in Early- to Mid-Season Corn. *Journal of the Science of Food and Agriculture*, **92**, 2611-2617. http://dx.doi.org/10.1002/jsfa.5700

[23] Sharma, L.K. and Franzen, D.W. (2014) Use of Corn Height to Improve the Relationship between Active Optical Sensor Readings and Yield Estimates. *Precision Agriculture*, **15**, 331-345. http://dx.doi.org/10.1007/s11119-013-9330-9

[24] Jackson, T.J., Chen, D., Cosh, M., Li, F., Anderson, M., Walthall, C., Doriaswamy, P. and Hunt, E.R. (2004) Vegetation Water Content Mapping Using Landsat Data Derived Normalized Difference Water Index for Corn and Soybeans. *Remote Sensing of Environment*, **92**, 475-482. http://dx.doi.org/10.1016/j.rse.2003.10.021

[25] Klees, R. and Massonnet, D. (1998) Deformation Measurements Using SAR Interferometry: Potential and Limitations. *Geologie en Mijnbouw*, **77**, 161-176. http://dx.doi.org/10.1023/A:1003594502801

[26] Rosen, P.A., Hensley, S., Joughin, I.R., Li, F.K., Madsen, S.N., Rodriguez, E. and Goldstein, R.M. (2000) Synthetic Aperture Radar Interferometry. *Proceedings of the IEEE*, **88**, 333-382. http://dx.doi.org/10.1109/5.838084

[27] Zebker, H.A. and Villasenor, J. (1992) Decorrelation in Interferometric Radar Echoes. *IEEE Transactions on Geoscience and Remote Sensing*, **30**, 950-959. http://dx.doi.org/10.1109/36.175330

[28] Krieger, G., Papathanassiou, K.P. and Cloude, S.R. (2005) Spaceborne Polarimetric SAR Interferometry: Performance Analysis and Mission Concepts. *EURASIP Journal on Advances in Signal Processing*, **2005**, Article ID: 354018. http://dx.doi.org/10.1155/ASP.2005.3272

[29] Lavalle, M. and Hensley, S. (2015) Extraction of Structural and Dynamic Properties of Forests from Polarimetric-Interferometric SAR Data Affected by Temporal Decorrelation. *IEEE Transactions on Geoscience and Remote Sensing*, **53**, 4752-4767. http://dx.doi.org/10.1109/TGRS.2015.2409066

[30] Anguela, T.P., Zribi, M., Baghdadi, N. and Loumagne, C. (2010) Analysis of Local Variation of Soil Surface Parameters with TerraSAR-X Radar Data Over Bare Agricultural Fields. *IEEE Transactions on Geoscience and Remote Sensing*, **48**, 874-881. http://dx.doi.org/10.1109/TGRS.2009.2028019

[31] Aubert, M., Baghdadi, N., Zribi, M., Douaoui, A., Loumagne, C., Baup, F., El Hajj, M. and Garrigues, S. (2011) Analysis of TerraSAR-X Data Sensitivity to Bare Soil Moisture, Roughness, Composition and Soil Crust. *Remote Sensing of Environment*, **115**, 1801-1810. http://dx.doi.org/10.1016/j.rse.2011.02.021

[32] Ulaby, F.T., Moore, R.K. and Fung, A.K. (1986) Microwave Remote Sensing Active and Passive-Volume III: From Theory to Applications. Artech House, Norwood.

[33] Saleh, K., Wigneron, J.P., Waldteufel, P., de Rosnay, P., Schwank, M., Calvet, J.C. and Kerr, Y.H. (2007) Estimates of Surface Soil Moisture under Grass Covers Using L-Band Radiometry. *Remote Sensing of Environment*, **109**, 42-53. http://dx.doi.org/10.1016/j.rse.2006.12.002

[34] Hajnsek, I., Jagdhuber, T., Schon, H. and Papathanassiou, K.P. (2009) Potential of Estimating Soil Moisture under Vegetation Cover by Means of PolSAR. *IEEE Transactions on Geoscience and Remote Sensing*, **47**, 442-454. http://dx.doi.org/10.1109/TGRS.2008.2009642

[35] Awal, M.A., Koshi, H. and Ikeda, T. (2006) Radiation Interception and Use by Maize/Peanut Intercrop Canopy. *Agricultural and Forest Meteorology*, **139**, 74-83. http://dx.doi.org/10.1016/j.agrformet.2006.06.001

[36] Coudert, B., Ottlé, C., Boudevillain, B., Demarty, J. and Guillevic, P. (2006) Contribution of Thermal Infrared Remote Sensing Data in Multiobjective Calibration of a Dual-Source SVAT Model. *Journal of Hydrometeorology*, **7**, 404-420. http://dx.doi.org/10.1175/JHM503.1

[37] Helander, C., Norgaard, P., Zaralis, K., Martinsson, K., Murphy, M. and Nadeau, E. (2015) Effects of Maize Crop Maturity at Harvest and Dietary Inclusion Rate of Maize Silage on Feed Intake and Performance in Lambs Fed High-Concentrate Diets. *Livestock Science*, **178**, 52-60. http://dx.doi.org/10.1016/j.livsci.2015.05.002

[38] Dente, L., Satalino, G., Mattia, F. and Rinaldi, M. (2008) Assimilation of Leaf Area Index Derived from ASAR and MERIS Data into CERES-Wheat Model to Map Wheat Yield. *Remote Sensing of Environment*, **112**, 1395-1407. http://dx.doi.org/10.1016/j.rse.2007.05.023

[39] Rinaldi, M., Satalino, G., Mattia, F., Balenzano, A., Perego, A., Acutis, M. and Ruggieri, S. (2013) Assimilation of COSMO-SkyMed-Derived LAI Maps into the AQUATER Crop Growth Simulation Model. Capitanata (Southern Italy) Case Study. *European Journal of Remote Sensing*, **46**, 891-908. http://dx.doi.org/10.5721/EuJRS20134653

[40] Duchemin, B., Fieuzal, R., Rivera, M.A., Ezzahar, J., Jarlan, L., Rodriguez, J.C., Hagolle, O. and Watts, C. (2015) Impact of Sowing Date on Yield and Water Use Efficiency of Wheat Analyzed through Spatial Modeling and FORMOSAT-2 Images. *Remote Sensing*, **7**, 5951-5979. http://dx.doi.org/10.3390/rs70505951

[41] Baup, F., Fieuzal, R. and Betbeder, J. (2015) Estimation of Soybean Yield from Assimilated Optical and Radar Data into a Simplified Agrometeorological Model. *IEEE International Geoscience and Remote Sensing Symposium*, Milan, 26-31 July 2015, 3961-3964. http://dx.doi.org/10.1109/igarss.2015.7326692

[42] Fieuzal, R. and Baup, F. (2015) Estimation of Sunflower Yield Using Multi-Spectral Satellite Data (Optical or Radar) in a Simplified Agro-Meteorological Model. *IEEE International Geoscience and Remote Sensing Symposium*, Milan, 26-31 July 2015, 4001-4004. http://dx.doi.org/10.1109/igarss.2015.7326702

[43] Van Niel, T.G. and McVicar, T.R. (2004) Determining Temporal Windows for Crop Discrimination with Remote Sensing: A Case Study in South-Eastern Australia. *Computers and Electronics in Agriculture*, **45**, 91-108. http://dx.doi.org/10.1016/j.compag.2004.06.003